Virology 527 (2019) 107–115

Contents lists available at ScienceDirect

Virology

journal homepage: www.elsevier.com/locate/virology

Neuronal transcriptomic responses to Japanese encephalitis virus infection with a special focus on chemokine CXCL11 and pattern recognition receptors RIG-1 and MDA5

Shu Pin Yu[a], Kien Chai Ong[b], David Perera[c], Kum Thong Wong[a,*]

[a] Department of Pathology, Faculty of Medicine, University of Malaya, Kuala Lumpur, Malaysia
[b] Department of Biomedical Science, Faculty of Medicine, University of Malaya, Kuala Lumpur, Malaysia
[c] Institute of Health and Community Medicine, University Malaysia Sarawak, Sarawak, Malaysia

ARTICLE INFO

Keywords:
Japanese encephalitis virus
Transcriptome
RNA microarray
Proinflammatory mediators
Neuronal infection
CXCL11
RIG-1
MDA5

ABSTRACT

Japanese encephalitis virus (JEV) causes central nervous system neuronal injury and inflammation. A clear understanding of neuronal responses to JEV infection remains elusive. Using the Affymetrix array to investigate the transcriptome of infected SK-N-MC cells, 1316 and 2737 dysregulated genes ($\geq 2/-2$ fold change, $P < 0.05$) were found at 48 hours post-infection (hpi) and 60 hpi, respectively. The genes were mainly involved in anti-microbial responses, cell signalling, cellular function and maintenance, and cell death and survival. Among the most highly upregulated genes (≥ 10 folds, $P < 0.05$) were chemokines CCL5, CXCL11, IL8 and CXCL10. The upregulation and expression of CXCL11 were confirmed by qRT-PCR and immunofluorescence. Pathogen recognition receptors retinoic acid-inducible gene-1 (RIG-1) and melanoma differentiation-associated protein 5 (MDA5) were also upregulated. Our results strongly suggest that neuronal cells play a significant role in immunity against JEV. CXCL11, RIG-1 and MDA5 and other cytokines may be important in neuropathogenesis.

1. Introduction

Japanese encephalitis virus (JEV) is an approximately 50 nm, spherical, enveloped virion containing a single strand, positive-sense RNA genome of 11 kb. The genome comprises 3′ and 5′ end untranslated regions, and an open reading frame that encodes for three structural proteins (C, prM, E) and seven non-structural proteins (NS1, NS2A, NS2B, NS3, NS4A, NS4B, NS5). JEV belongs to the family *Flaviviridae* and genus *Flavivirus* (Misra and Kalita, 2010; Unni et al., 2011), which includes the West Nile virus (WNV), dengue virus (DENV) and tick-borne encephalitis virus (TBEV).

JEV is one of the leading causes of mosquito-borne encephalitides in the world. An annual estimated incidence of about 68,000 cases of Japanese encephalitis (JE), resulting in 13,600–20,400 deaths was reported in affected areas (WHO, 2015). The fatality rate ranges from 25% to 50%, and more than 50% of survivors develop permanent neurological complications (Libraty et al., 2002). Nevertheless, most JEV infections are subclinical, with only a chance of 1:25–1:1000 of developing into symptomatic JE (Solomon and Vaughn, 2002). The virus is maintained in an enzootic cycle between birds, swine and mosquitoes (*Culex*.sp). Human beings are incidental dead-end hosts, in which there is no significant post-infection viremia (Tiroumourougane et al., 2002).

JE is a meningoencephalitis characterized by perivascular cuffing and parenchymal infiltration by inflammatory cells with microglial nodule formation, edema, neuronophagia and necrosis in the central nervous system (CNS) (German et al., 2006). The neuron is the main viral target as evidenced by the neuronal localization of viral antigens and RNA in the cerebral grey matter, thalamus, brainstem, cerebellum, hippocampus, spinal cord and other parts of the CNS (German et al., 2006; Wong et al., 2012). A positive correlation between fatality rate and cytokine levels of IFN-α, IFN–γ, TNF-α, IL2, 4, 6 and 8 in the cerebrospinal fluid (CSF) and serum had been demonstrated (Babu et al., 2006; Ravi et al., 1997; Singh et al., 2000; Winter et al., 2004), suggesting that these inflammatory mediators have significant roles in neuropathogenesis. At present, there is little information with regards to direct immune responses from viral-infected neurons in general, and in particular, JEV-infected neurons.

In order to study early neuronal responses to JEV infection, the microarray technology was used to characterize the entire

* Corresponding author.
E-mail address: wongkt@ummc.edu.my (K.T. Wong).

https://doi.org/10.1016/j.virol.2018.10.015
Received 6 July 2018; Received in revised form 1 October 2018; Accepted 16 October 2018
Available online 24 November 2018
0042-6822/

transcriptomic profile. Since our preliminary data demonstrated a high and early upregulation of proinflammatory gene transcripts, we focussed on innate immune responses. Moreover, WNV infection of human neuroblastoma cells was found to induce neuronal death and astrocytic activation by neuronal release of IL-1β, TNF-α, IL6 and IL8 (Kumar et al., 2010). Interferon inducible chemokines CXCL10 and CXCL11, was reported to be upregulated in the CSF of TBE patients (Lepej et al., 2007; Zajkowska et al., 2011), as well as in mouse brains infected with WNV (Venter et al., 2005). *In vitro* and *in vivo* neuronal and astrocytic CXCL10 production have been demonstrated in JEV infected neuroblastoma cells as well as in mouse models (Bhowmick et al., 2007; Gupta and Rao, 2011; Nazmi et al., 2011). To date, there is no concrete evidence demonstrating the production of CXCL11 from JEV-infected neurons. Like CXCL10, CXCL11 is a T cell chemoattractant and may play an important role in JE.

First discovered in 1987, chemokines are chemoattractant cytokines of molecular weights ranging from 8 to 12 kDa (Bendall, 2005). CXCL11, also known as IFN-inducible T cell α-chemoattractant or IFN-γ inducible protein 9, is a distinct chemokine that possesses a high affinity for CXCR3 receptors and exhibits potent chemotactic activity for activated Th1 lymphocytes (CD8 activated T cells, natural killer cells). It is thus one of the important downstream effectors of inflammatory signalling in innate immunity (Cole et al., 1998). As part of early innate immunity, detection of viruses or other pathogens by pattern recognition receptors (PRRs) such as retinoic acid-inducible gene-1 (RIG-1) and melanoma differentiation-associated protein 5 (MDA5) occurs. Subsequently, PRR activation leads to synthesis and activation of downstream cytokines, chemokines, cell adhesion molecules and immunoreceptors (Mogensen, 2009). Involvement of both systemic RIG-1 and MDA5 following WNV (Errett et al., 2013; Fredericksen et al., 2008) and DENV (Nasirudeen et al., 2011) infection have been demonstrated. To date, there is little information regarding PRR upregulation in JEV-infected neurons. Thus, the aim of this study is to investigate neuronal responses to JEV infection in general, and in particular, focus on CXCL-11, RIG-1 and MDA5 as important mediators of innate immunity.

2. Methods and materials

2.1. Cell and virus culture

Human neuroepithelioma cells (SK-N-MC; ATCC, USA) and *Aedes albopictus* cells (C6/36; ATCC, USA) were cultured in Dulbecco's Modified Eagle Medium high glucose (DMEM) and Roswell Park Memorial Institute medium (RPMI 160) (Sigma-Aldrich, USA), respectively, supplemented with 10% fetal bovine serum (FBS) (HyClone, Fisher Scientific, USA) and gentamycin. The JEV prototype (Nakayama strain) and the clinical isolate (CNS138/9) (Henry Sum, 2015) were propagated and titrated in C6/36 cells. Virus titre was determined using the cell culture infectious dose 50% ($CCID_{50}$) method, as described previously, with minor modifications (Schoepp and Beaty, 1984). Briefly, C6/36 cells were seeded into 96-well plates and cell monolayers were inoculated with 10 fold serial dilutions of virus, with 4 replicates for each dilution. The infected cells were incubated at room temperature, and on the 7th day post infection, the cells were fixed with ice cold methanol. Viral antigens were detected by immunohistochemistry (IHC) using anti-JEV mouse polyclonal antibody (Jath-160; courtesy of Dr. Takasaki, National Institute of Infectious Diseases, Japan) to indicate infection since JEV infected C6/36 cells do not show obvious cytopathic effects (CPE). Virus titres were calculated using the Karber's method (Kärber, 1931).

2.2. JEV infection in SK-N-MC cells

JEV infectivity in human neuronal cell lines was first evaluated in two human neuroblastoma cell lines, SK-N-SH and SK-N-MC at multiplicity of infection (MOI)s of 5, 10, 15 and 20. Since SK-N-MC cells, showed a higher susceptibility to infection (> 50% infection at 48 hpi) at MOIs of 5 and 10 and there was no significant CPE observed in control cells exposed to equal amounts of UV-inactivated viruses, SK-N-MC cells and an MOI of 10 were used throughout this study.

Aliquots of 4×10^5 SK-N-MC cells were seeded into 12-well plates and were infected with the JEV at MOI of 10 (4×10^6 $CCID_{50}$) the next day. Uninfected cell controls received DMEM/5% FBS (volume equal to the virus aliquot). Following an hour pre-absorption at 36 °C, unbound viruses were removed by washing with phosphate buffered saline (PBS, pH7.4) and fresh DMEM/5% FBS was added. Cell cultures were further incubated in 36 °C and were monitored daily.

2.3. One-step virus growth curve

To determine the one-step growth curve of JEV infection in SK-N-MC cells, cell-free supernatants containing extracellular viruses were collected at 24, 48, 60, 72 and 96 hpi. Infected cells containing intracellular viruses were washed thrice with PBS, and then collected in fresh DMEM/5% FBS after three freeze-thaw cycles. Intracellular and extracellular virus titres ($CCID_{50}$/ml ± SD) were then determined from three independent experiments.

2.4. IHC to detect viral antigens

To detect viral antigens by IHC, infected SK-N-MC cells were harvested at 24, 48, 60, 72 and 96 hpi and fixed in ice cold methanol. Endogenous peroxidase blocking was performed before overnight incubation with anti-JEV antibody (1:5000 dilution, 4 °C). The secondary Envision HRP conjugated goat anti-mouse antibody (Dako, Denmark), diluted 1:1 in Tris-buffered saline (TBS, pH 7.6) was added and incubated for 30 mins at room temperature. Chromogen development was achieved using 3,3′-diaminobenzidine (Dako, Denmark). The cells were counterstained with Harris hematoxylin. Washes in between steps were done using TBS, pH7.6.

2.5. Flow cytometry to determine the percentages of infected cells

Flow cytometry was performed to determine the percentage of infected cells at 24, 48, 60, 72 and 96 hpi by viral antigen detection. After harvesting, cells were fixed with FluoroFix Buffer, (Biolegend, San Diego, CA), permeabilized with 0.1% Triton-X, and incubated with anti-JEV antibody (1:500 dilution, 30 min), followed by the secondary antibody (Alexa Fluor 488 goat anti-mouse IgG; 1:500 dilution; Invitrogen, USA) for 30 min. The percentages of viral antigen-positive cells from 3 independent sets of experiments were determined using the FACSCANTO II (BD Bioscience, USA) and presented as % ± SD.

2.6. Gene expression profiling of infected SK-N-MC cells

Total RNA from uninfected and JEV-infected SK-N-MC cells were extracted at 48 and 60 hpi using the RNeasy Plus Mini kit (QIAGEN, Germany), following the manufacturer's protocol. The RNA integrity for each RNA sample was determined using RNA nanochips (Agilent, USA). Total RNAs with A260/A280 and A230/A280 readings of > 1.9 and RIN values of > 9 were used for gene expression profiling using the Human PrimeView Array GeneChip (Affymetrix, USA) that interrogates a total of 49,395 gene transcripts. The RNA targets were labelled using the GeneChip 3′ IVT Plus kit (Affymetrix, USA) according to the manufacturer's protocol. In brief, 100 ng total RNA were reverse transcribed to obtain the first strand cDNA, which were then used as templates to synthesize the second cDNA strand. This was followed by *in vitro* transcription to synthesize copies of biotin-labelled amplified RNA (aRNA) and magnetic-bead purification. The aRNA was heat fragmented with Array Fragmentation buffer provided with the GeneChip 3′ IVT Plus kit before hybridization onto Human PrimeView arrays using

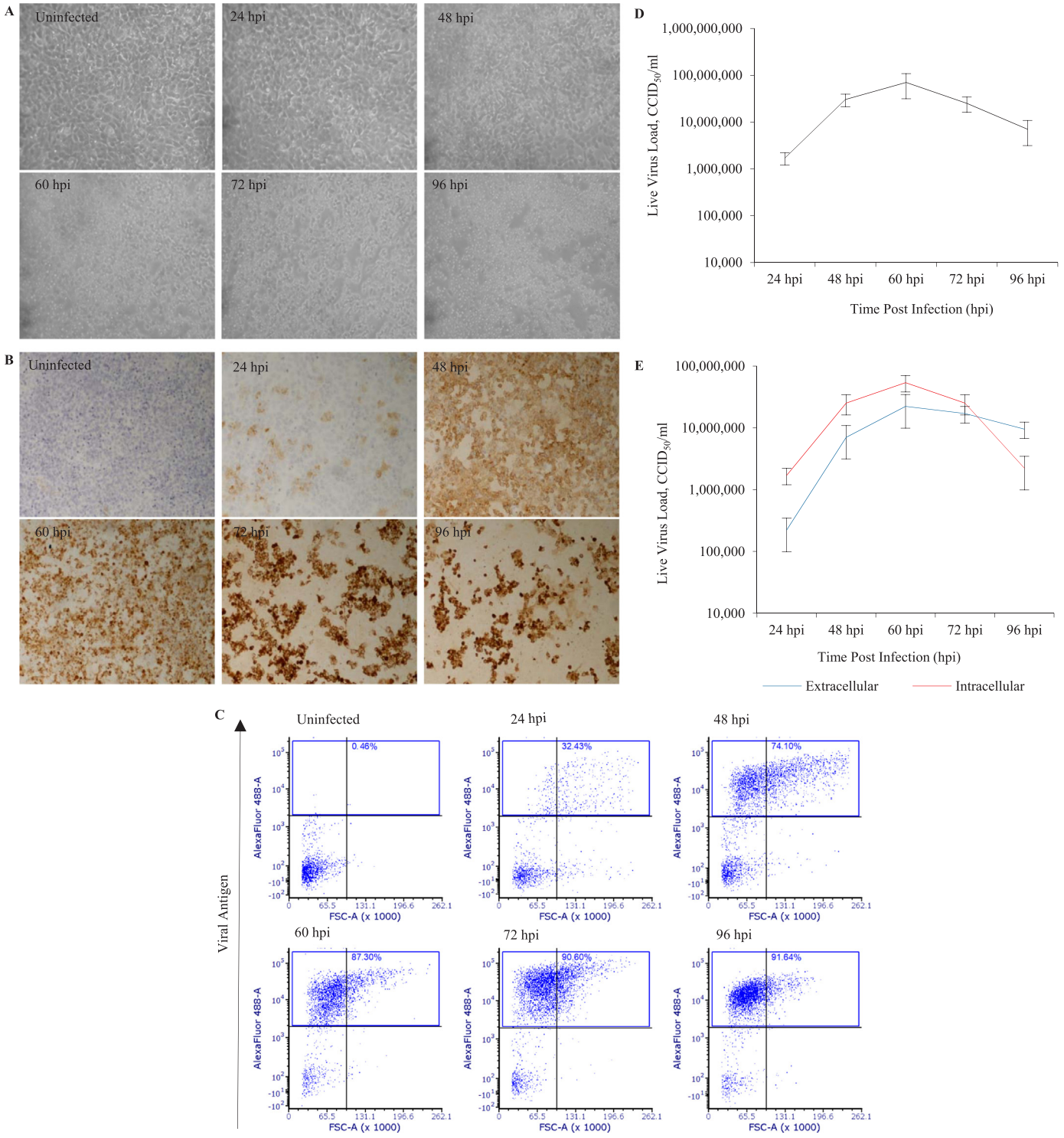

Fig. 1. JEV infection of SK-N-MC cells. (A) Infected SK-N-MC cells (magnification: 10x objective lens) from 24 hpi to 96 hpi. Cell distortion was observed starting at 48 hpi, and cell detachment from 72 hpi onwards. (B) Immunohistochemical staining for viral antigens confirmed increasing infection from 24 hpi to 72 hpi. The apparent decrease of viral antigens at 96 hpi is due to cell loss from detachment (magnification: 10x objective lens). (C) Representative flow cytometry dot plots showing increasing percentages of infected cells from 24 hpi to 96 hpi. Corresponding JEV replication kinetics (one-step growth curve) for total virus (D) and intracellular and extracellular viruses separately (E) are shown as $CCID_{50}$/ml ± SD. All data presented above were derived from three separate experimental replicates.

the GeneChip Hybridization, Wash and Stain Kit (Affymetrix, USA) at 45 °C for 16 h at 60 rpm. After hybridization, the arrays were washed, stained and analyzed using the GeneChip Scanner 3000 with the AGCC scan control software (Affymetrix, US).

Each data set were pre-processed, normalized and analyzed using Expression Console and Transcriptome Analysis Console, v3 (Affymetrix, USA) to obtain sets of differentially expressed genes and to generate heatmaps showing an overview of the patterns of gene dysregulations at 48 hpi and 60 hpi. Raw expression data were background corrected, quantile normalized and summarized using Robust Multichip

Averaging (Affymetrix, USA) to account for any systemic variations occurring during the microarray experiments. Baseline data transformation was conducted wherein log-summarized values were calculated for all the samples. Three data sets from biological replicates of JEV-infected and uninfected control experiments, respectively, were analyzed.

Using ANOVA, dysregulated genes were defined as fold changes of ≥ 2 or ≤ -2 and P-values < 0.05 were the cut-off points of significance. A Pearson's correlation analysis was done to examine the relationship between genes derived from the 2 post infection time points. Venn diagrams showing the amount of overlap genes and genes that were uniquely upregulated or downregulated at both the post infection time points were derived using the web base GeneVenn software (Pirooznia et al., 2007). Gene ontology and pathway enrichment analysis was performed with Ingenuity Pathway Analysis, IPA (QIAGEN, Germany) to study the biological functionality and to explore the involvement of the differentially expressed genes sets in various known pathways. The most significant functional processes of biological importance were identified upon mapping the gene list to the IPA Knowledge Base, with IPA calculated Fisher's exact test of $p < 0.05$ as the cut-off points of significance. Activation z-score of > 2 or < -2 were used as cut-off points to predict likely activation (positive values) or inactivation (negative values) of a biological function.

2.7. Validation of microarray gene expression data

Quantitative real time PCR (qPCR) was carried out using commercially-available ABI Taqman Gene Expression Assays (Applied Bioscience, USA) to validate the gene expression changes of CXCL11, CXCL10, IL8, RIG-1 (or DDX58) and MDA5 (or IFIH1). Ribosomal protein lateral stalk subunit P0 (RPLP0) and Ubiquitin C (UBC) were used as endogenous reference genes. Pairwise variation of RPLP0 and UBC determined as geNorm's average stability measure, M was 0.258, giving an indication that their relative expression was not altered by JEV infection. The acceptance cut-off of stability was set as $M < 0.5$. The commercially available ABI gene expression product codes were summarized as follows: IL8 (HS 00174103_ml), CXCL10 (HS 01124252_g1), CXCL11 (HS_04187682_g1), DDX58/RIG-1 (HS 01061436_m1), IFIH1/MDA5 (HS 00223420_m1), UBC (HS 00824723_m1), RPLP0 (HS 99999902_m1). The thermal cycler conditions for all assayed reactions were: holding stage at 50 °C, 2 min; 95 °C, 20 s, followed by 40 cycles of denaturation and annealing at 95 °C, 3 s and 60 °C, 30 s, respectively. The amplification efficiencies of all the sampled assays mentioned above were more than 95%. All samples were assayed in triplicate. In addition to 48 and 60 hpi, relative quantification qPCR was also performed on uninfected and JEV infected SK-N-MC at 24 and 72 hpi for CXCL11, RIG-1 and MDA5 to determine the gene transcript kinetics further.

2.8. Double immunofluorescence to localize CXCL11 and viral antigens in SK-N-MC cells

To investigate co-localization of cellular CXCL11 and viral antigens, 4×10^5 of SK-N-MC cells were seeded on a coverslip overnight before infection with JEV (MOI 10; Nakayama and CNS138/9). Infected and uninfected cells were methanol-fixed at 48 hpi and blocked with normal goat serum before overnight incubation with anti-CXCL11 (Abcam, UK; 1:400 dilution) and anti-JEV (1:2500 dilution) antibodies at 4 °C. Primary antibodies were detected using Alexa flour 488 goat anti-mouse and Alexa flour 594 goat anti-rabbit secondary antibodies (Invitrogen, USA). Cells were counterstained with DAPI (Invitrogen, USA) before mounting with paramount aqueous mounting medium (Dako, Denmark). The cells were viewed under High Resolution Upright Compound Leica DM6000B microscope.

3. Results

3.1. SK-N-MC cells are highly permissive to JEV infection

Progressive CPE following JEV infection of SK-N-MC cells at MOI of 10 was observed starting at 48 hpi (Fig. 1A). These changes correlated with the increasing amounts of viral antigens as detected by IHC (Fig. 1B), and increasing percentages of infected cells by flow cytometry (Fig. 1C). Significant percentage increases of infected cells were seen from 24 hpi to 48 hpi ($P = 0.003$), and from 48 hpi to 60 hpi ($P = 0.020$). Significant increase in total (intracellular and extracellular) viral titres was observed from 24 hpi to 48 hpi ($P = 0.033$), peaking at 60 hpi, and reaching a plateau thereafter (Fig. 1D, E). These results confirmed that SK-N-MC cells were highly supportive of JEV infection and replication.

3.2. Gene expression profiles of infected SK-N-MC cells

The microarray data was deposited in the NCBI Gene Expression Omnibus (GEO) under the data accession number: GSE115167 following the Minimum Information About a Microarray Experiment, MIAME guideline (Brazma et al., 2001). Based on our data, the gene expression profile at 48 hpi was assumed to represent early infection, whereas 60 hpi represented a later time point when infection was fully established. Moreover, the Pearson's correlation analysis indicated that JEV-infected and uninfected SK-N-MC cells exhibited divergent expression profiles that became more prominent at 60 hpi (data not shown). Out of the total of 49,395 interrogated transcripts in the array chip, 1316 and 2737 genes representing about 2.7% and 5.5%, respectively, were significantly dysregulated (fold changes of ≥ 2 or ≤ -2, and P-values < 0.05) at 48 hpi and 60 hpi, respectively. Most were upregulated genes, with a total of 1067 and 1565 genes at 48 hpi and 60 hpi, respectively, while 249 and 1172 genes were downregulated at 48 hpi and 60 hpi, respectively. Fig. 2 shows the 689 genes upregulated at both 48 hpi and 60 hpi, while only 175 genes were downregulated at these time points. Schematic heatmaps showing an overview of the pattern of gene dysregulations at 48 hpi and 60 hpi are shown in Supplementary Fig. 1.

IPA gene function enrichment analysis of all the upregulated genes in the disease and biofunction group generally fall into three categories: A) disease and disorders, B) molecular and cellular functions, and C) physiological system development and functions (Fig. 3). In the disease and disorders category, genes were most highly associated with antimicrobial and inflammatory responses.

The disease and biofunction genes with the highest upregulation (defined as fold changes ≥ 10 and $P < 0.05$) were further analyzed using IPA activation z-scores to predict their activation states. Seven out of 8 categories with positive z-scores or predicted activation at both time points were found to be involved in general inflammatory responses. These gene subsets included 1) migration of mononuclear

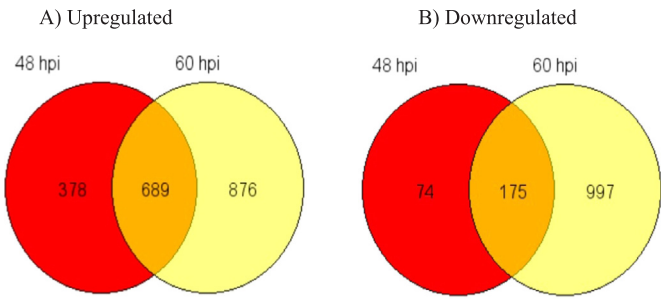

Fig. 2. Venn diagrams summarizing the number of genes that are upregulated and downregulated (fold changes ≥ 2 and ≤ -2, $P < 0.05$) at 48 hpi and 60 hpi. Among upregulated and downregulated genes, 689 genes and 175 genes, respectively, were dysregulated at both time points.

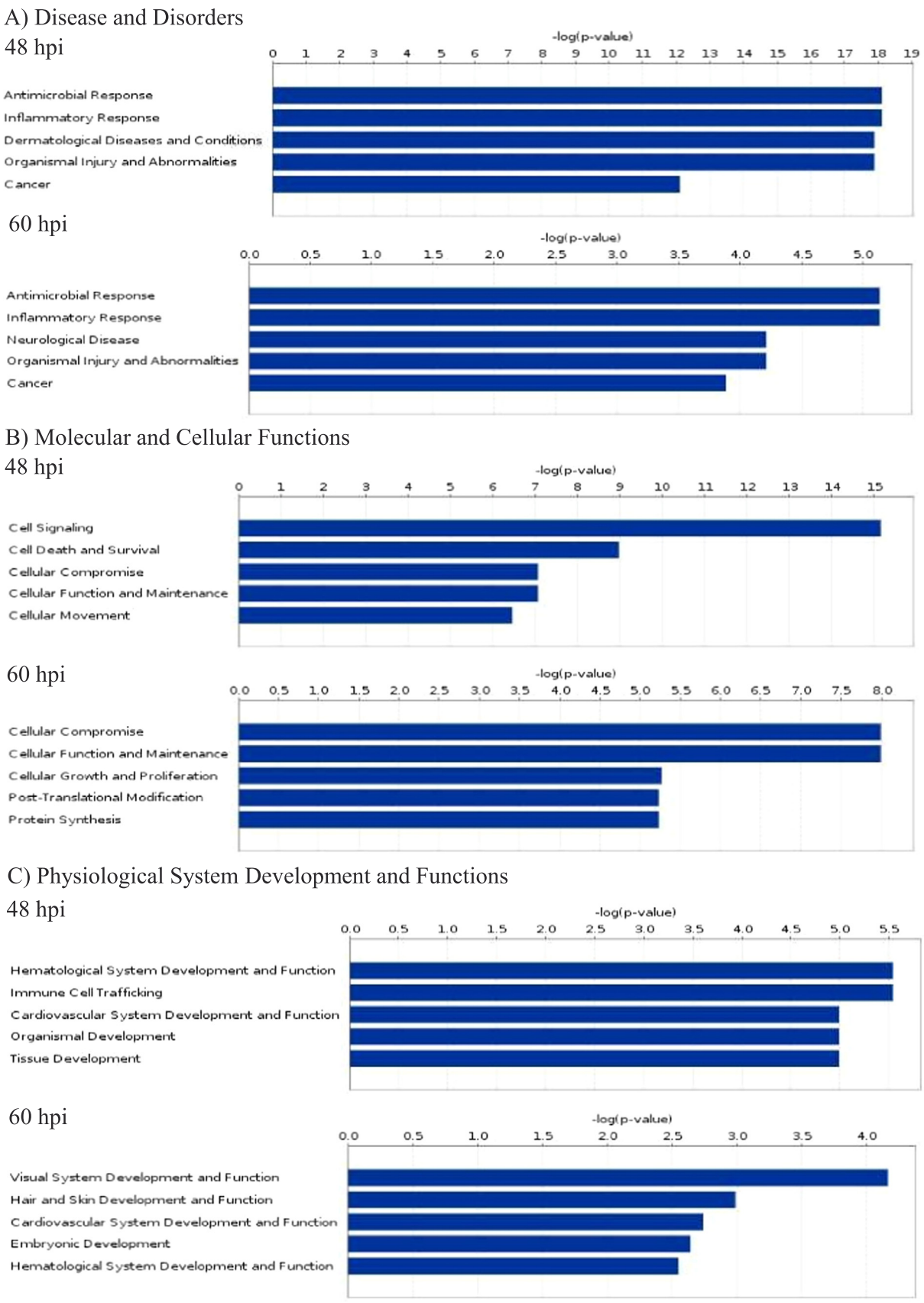

Fig. 3. An overview of the IPA analysis of all upregulated genes (≥ 2 folds) involved in disease and biofunction at 48 and 60 hpi, categorized as (A) Disease and Disorders, (B) Molecular and Cellular Functions, and (C) Physiological System Development and Functions. The significance of association between the analyzed genes and their assigned categories were determined by IPA calculated Fisher's exact test with P-values < 0.05 as the cut-off point of significance. In the Disease and Disorders category (A), the two highest sub categories were genes associated with antimicrobial and inflammatory responses.

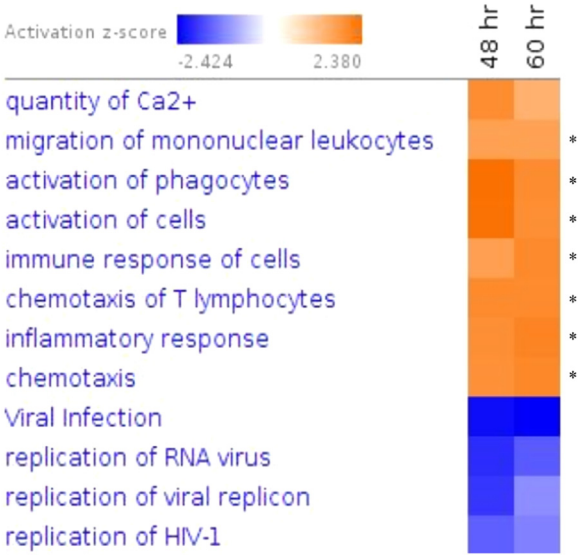

Fig. 4. IPA analysis of highly upregulated genes (fold changes ≥ 10, and P-values < 0.05) involved in disease and biofunction at 48 hpi and 60 hpi. Predictions of the activation states of these gene subsets are shown in the blue-brown scale on the right: brown color denotes predicted activation; blue color denotes predicted inhibition. Overall, gene subsets involved with inflammatory responses* showed activation (brown color) whereas, viral infection/replication showed inhibition (blue color) at both time points.

Table 1
Chemokine and PRR gene upregulations at 48 hpi and 60 hpi.

Genes	48 hpi		60 hpi	
	Fold changes	P-values	Fold changes	P-values
Cytokines/Chemokines				
IFNB1	739.8	0.000428	81.5	0.001706
CCL5	139.4	0.002627	27.6	0.001476
CXCL11	102.4	0.000255	51.5	0.000839
IL8	102.4	0.000228	14.4	0.005771
CXCL10	37.8	0.000022	57.7	0.001840
Pattern Recognition Receptors				
RIG-1	17.3	0.000355	5.8	0.001341
MDA5	5.9	0.000169	2.7	0.020139

Chemokine genes were among the most highly upregulated with fold changes of more than 10 folds at both time points.

leukocytes, 2) activation of phagocytes, 3) activation of cells, 4) immune response of cells, 5) chemotaxis of T lymphocytes, 6) inflammatory response and, 7) chemotaxis (Fig. 4). These highly upregulated genes are closely interlinked with each other (Supplementary Fig. 2). Highly associated genes included IFNB1 and chemokine genes CCL5, CXCL11, IL8 and CXCL10, which were prominently involved in many of these categories (Table 1).

In the "immune response of cells" subset, the PRR, RIG-1 was upregulated 17.3 folds and 5.8 folds at 48 hpi and 60 hpi, respectively (Table 1) (Array data accession number: GSE115167; RIG-1 is also known as DDX58). The closely related RIG-like PRR, MDA5 was also significantly upregulated 5.9 folds and 2.7 folds at 48 hpi and 60 hpi, respectively (Table 1) (Array data accession number: GSE115167; MDA5 is also known as IFIH1). This is consistent with the role of PRRs to detect RNA viruses leading to downstream type I interferon and proinflammatory cyto/chemokine production and activation. Thus, IFNB1, CXCL11, IL8, CXCL10, and CCL5 were found to be among the most highly upregulated genes.

Although the number of downregulated genes was not as high as upregulated genes, significantly downregulated genes at 60 hpi were approximately 5 times more than at 48 hpi. At 48 hpi, downregulation of genes associated with cellular functions such as cellular growth and proliferation, cell cycle, tissue morphology, DNA replication, recombination and repair, and connective tissue development and function, tissue development, organismal injury and abnormalities, tissue development, cellular movement, cellular development were observed. At 60 hpi, prominent downregulation of genes involved in cell death and survival, cell morphology, nervous system development and function, organismal development, assembly, organization and development, tissue development, organismal injury and abnormalities, tissue development, cellular movement, cellular development were observed.

3.3. Taqman qRT-PCR confirmation of microarray results

Since the microarray results suggest a robust induction of innate immune responses in infected neurons, we sought to validate expressions of several key genes involved. Gene expressions of CXCL11, CXCL10, IL8, RIG-1 and MDA5 post infection were validated using Taqman qRT-PCR. In general, the results showed the same relative upregulation as the microarray data, although fold differences were not identical between the two methods of analysis (Fig. 5A).

In order to confirm sustained upregulation of CXCL11, RIG-1 and MDA5, two additional time points at 24 hpi and 72 hpi were also investigated by qPCR. CXCL11 relative to uninfected cells was confirmed to be significantly upregulated as early as 24 hpi (17.2 folds) and 72 hpi (49.8 folds) (Fig. 5B). At 24 hpi, RIG-1 and MDA5 upregulation was minimal (< 2 folds). From 48 hpi to 72 hpi, RIG-1 and MDA5 were upregulated more than 2 folds. RIG-1 upregulation ranged from 5.4 folds to 13.4 folds, whereas MDA5 ranged from 2.8 folds to 4.3 folds (Fig. 5B). Overall, RIG-1 upregulation was higher than MDA5 at all time points.

3.4. CXCL11 expression

Co-localization of viral antigens (Nakayama and CNS138/9 strains) and CXCL11 was demonstrated by double immunofluorescence using anti-JEV and anti-CXCL11 antibodies in JEV-infected cells. A majority of the cells were viral antigen-positive by 48 hpi. Positive CXCL11 signals mainly colocalized in the cytoplasm of JEV-infected cells. Uninfected cells were negative for both viral antigens and CXCL11 (Fig. 6).

4. Discussion

Viral infections in the CNS often invoke distinct proinflammatory mediator profiles, and neurons have been shown to be immunologically active (Lampron et al., 2013). Like other well-established neurotropic flaviviruses such as WNV and TBEV, JEV specifically targets CNS neurons during infection. Thus, neuronal cell responses to JEV infection, particularly innate immunity responses, are of considerable interest and significance. The transcriptome derived from infected human SK-N-MC cells, which was confirmed to be highly susceptible to JEV infection, showed numerous upregulated genes involved with immunity. We found that both PRRs (RIG-1 and MDA5) were upregulated. The associated downstream proinflammatory mediators such as IFNB1, IL8, CCL5, CXCL10 and CXCL11 were confirmed as the most highly upregulated genes (Fig. 5, Table 1). Moreover, CXCL11 was shown to be expressed in JEV-infected cells (Fig. 6).

PRRs are the initial drives towards the initiation and modulation of anti-microbial responses, and active cytoplasmic and endoplasmic PRRs can be found in neurons. RIG-1 and MDA5 both belong to the same RIG-like receptor family. Previously, RIG-1 was found to be expressed in JEV-infected murine neuroblastoma cells, BALB/C mouse brains, and primary cultures of cortical neurons resulting in the release of p38MAPK and other cytokines, and NFkB activation. Interestingly, upon blocking of RIG-1, several downstream proinflammatory mediators/effectors such as the IL-6, IL-12p70 (IL-12), monocyte

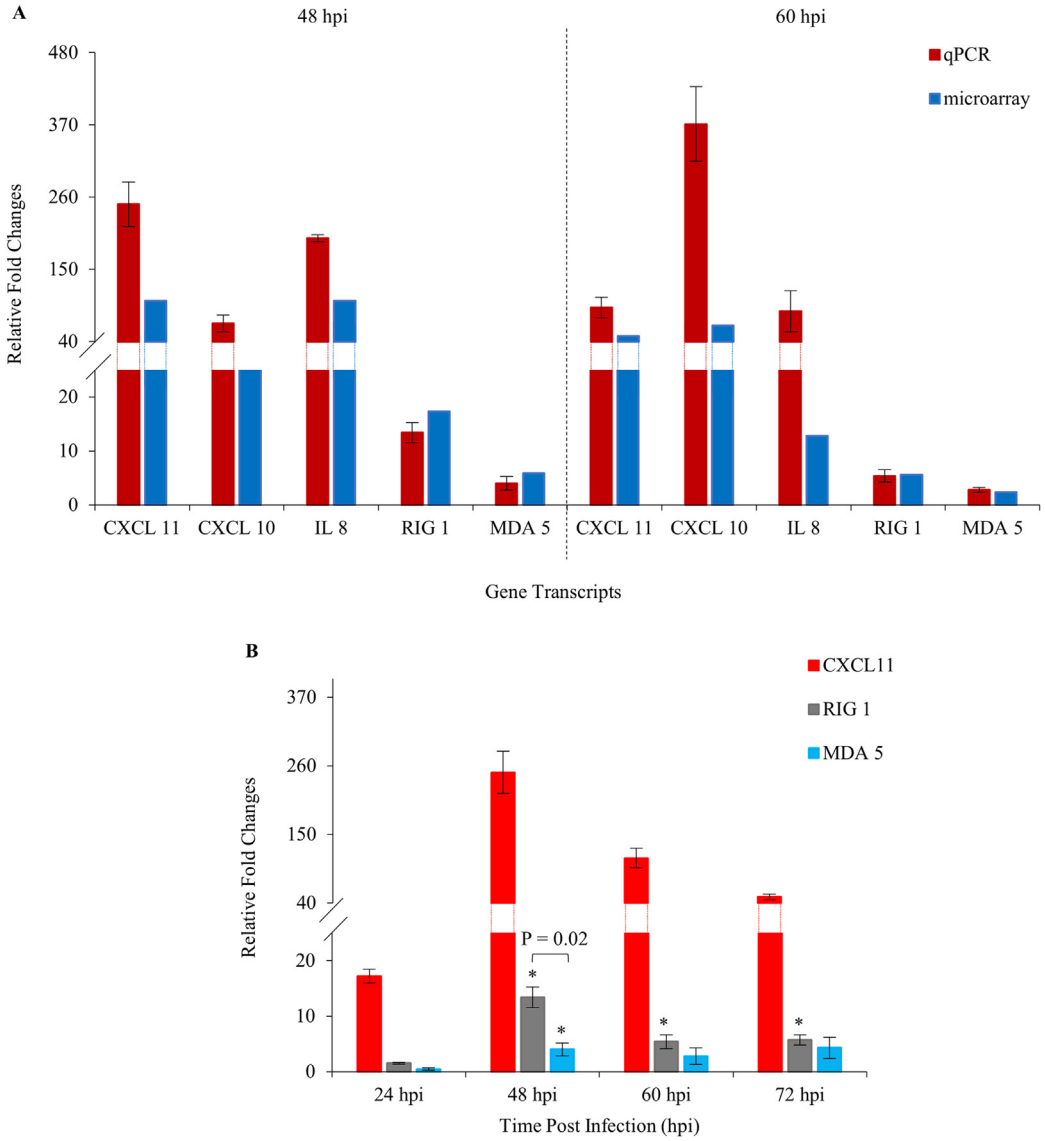

Fig. 5. (A) Relative fold changes of CXCL11, CXCL10, IL8, RIG-1 and MDA5 genes at 48 hpi and 60 hpi analyzed by qPCR and microarray. Fold change variations and trends were generally similar. (B) CXCL11, RIG-1 and MDA5 gene upregulations from 24 hpi to 72 hpi by qPCR. CXCL11 were highly and significantly upregulated at all time points: 24 hpi (17.2 folds), 48 hpi (249.2 folds), 60 hpi (112.0 folds), and 72 hpi (49.8 folds). At 24 hpi, RIG-1 (1.5 folds) and MDA5 (0.5 folds) upregulation were low. Thereafter, at all time points, higher and significant increases of RIG-1 compared to the 24 hpi level were observed. MDA5 increase was significant only at 48 hpi compared to 24 hpi level. RIG-1's fold changes at 48, 60 and 72 hpi were 13.4, 5.4, 5.7, respectively; MDA5 fold changes were 4.0, 2.8, 4.3. The * denotes significant differences ($P < 0.05$) compared to fold changes at 24 hpi. At 48 hpi, RIG-1 was significantly higher than MDA5 ($P = 0.02$). For qPCR, target genes were normalized to the levels of the endogenous reference genes. Relative fold changes of the target genes were calculated based on $2^{-\Delta\Delta ct}$ method (Livak and Schmittgen, 2001) and were presented as relative fold changes ± SD. All data above were from three experimental replicates.

chemoattractant protein-1, CXCL10 and TNF-α were decreased but not completely absent, suggesting a possibility for the involvement of other PRRs (Nazmi et al., 2011). Our results suggest that MDA5 may be one of them. However, in another study, MDA5 was not found to be upregulated in JEV-infected Neuro2a murine neuroblastoma cells and intracerebrally-inoculated suckling mouse brains (Fadnis et al., 2013). Nevertheless, MDA5 was transcriptionally co-expressed with Toll-like Receptor 2 in adult mouse brains. Co-involvement of systemic RIG-1 and MDA5 in the detection of WNV RNA had been shown in WNV infection of RIG-1, MDA5 and double RIG-1 and MDA5 knockout mice (Errett et al., 2013). Involvement of both RIG-1 and MDA5 in JE, however, has not been demonstrated before. In our study, both RIG-1 and MDA5 PRRs were upregulated suggesting that flaviviral CNS infections may involve these 2 PRRs. Moreover, upregulation of both RIG-1 and MDA5 may suggest a synergistic function. JEV uncapped genomes and dsRNA replication intermediates, which accumulate rapidly during active viral replication could be ligands to both RIG-1 and MDA5 (Kato et al., 2006; Loo and Gale, 2011). Differences in MDA5 expression in studies using murine neuroblastoma cells and mouse models (Fadnis et al., 2013) could be due to species variation and/or differences between mouse and human cells used in our study. More studies would be needed to confirm and better define the involvement and interrelation of these PRRs in JE.

Recent studies have demonstrated the emerging roles of the closely-related chemokines CXCL10 and CXCL11 in flaviviral neuropathogenesis. Both CXCL10 and CXCL11 were upregulated in mouse brains infected with highly neuroinvasive WNV strains (Venter et al., 2005). Neuronal secretion of CXCL10 was suggested to have a potential role in neuroprotection by enhancing CD8 + T cells trafficking into the CNS (Klein et al., 2005). CXCL10 upregulation and expression has been demonstrated in JEV-infected murine neuroblastoma cells, subcutaneously-infected mouse brains (Gupta and Rao, 2011), and even astrocytes in intracerebrally-infected BALB/C mice (Bhowmick et al., 2007). On the other hand, CXCL11 expression in JEV infection is more equivocal. Gupta et al., 2010b demonstrated insignificant CXCL11 gene dysregulation in JEV-infected murine neuroblastoma cells (Gupta et al., 2010b), but CXCL11 was shown to be upregulated in the brains of subcutaneously-infected mice (Gupta et al., 2010a). However, the cellular source of CXCL11 in the brains was not investigated. In our study, the high CXCL11 gene and antigenic expressions in JEV-infected SK-N-MC cells, support the notion that CXCL11 induction can occur in infected neurons very early on. Since CXCL11 share the same CXCR3 chemokine receptor with CXCL10, and exhibits potent chemotactic activity for activated Th1 lymphocytes, neurotrophils, monocytes and natural killer cells, CXCL11 may also play an important role as chemoattractant for critical protective immune cells into the CNS. This is

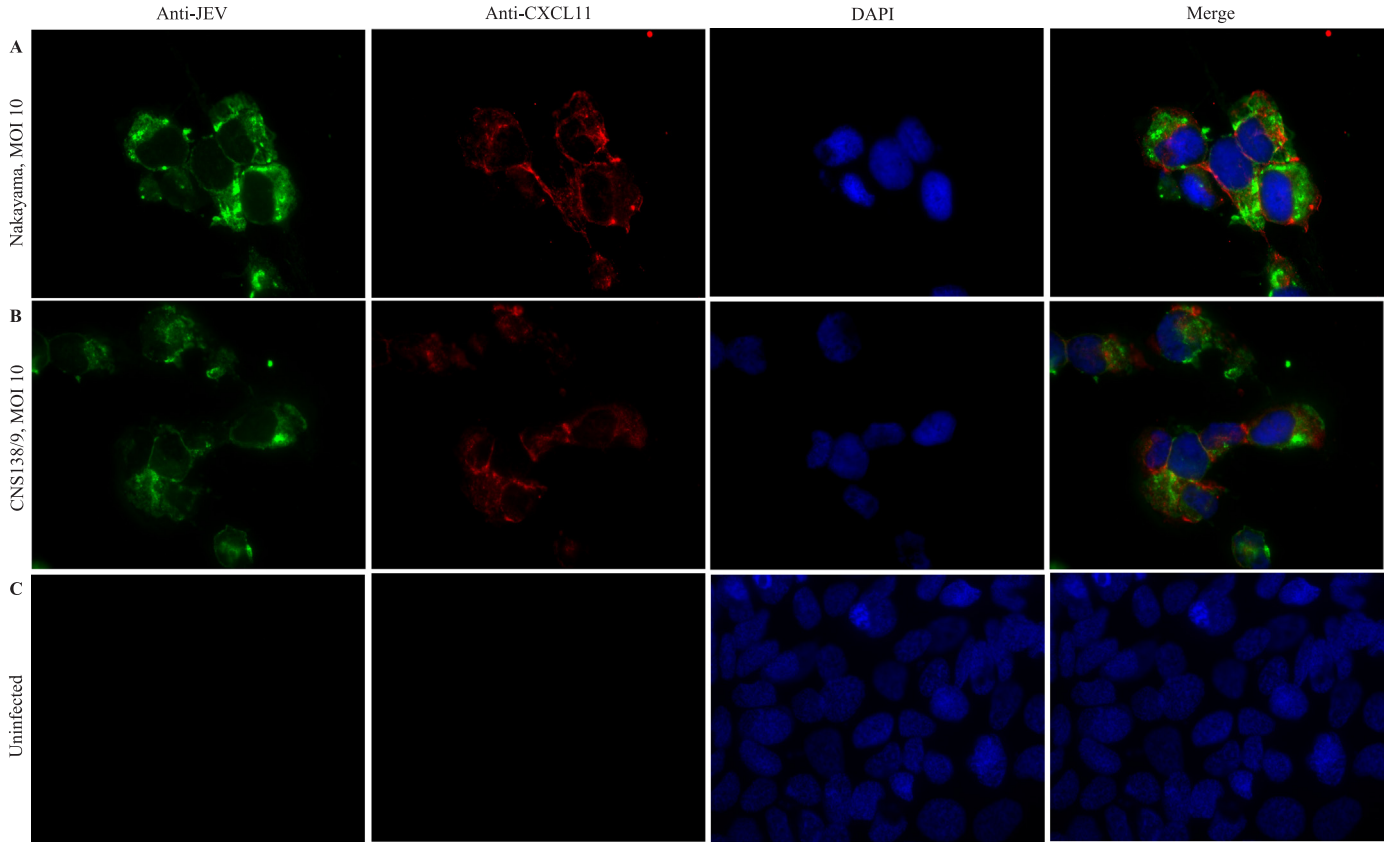

Fig. 6. Immunofluorescence for CXCL11 and JEV antigens in SK-N-MC cells at 48 hpi, showing colocalization of CXCL11 and viral antigens of the Nakayama prototype (A) and CNS138/9 clinical isolate (B). Green: 488 nm (anti-JEV), Red: 594 nm (anti-CXCL11), and Blue: 376 nm (DAPI) (magnification: 100 ×, oil immersion objective lens).

consistent with JE neuropathology, which is characterized by severe neuroinflammation and the high proportion of inflammatory infiltrates comprising mainly of macrophages, CD4 and CD8-activated T cells (German et al., 2006).

CXCL10 and CXCL11 chemokines have been shown to be increased in the CSF of TBE patients (Lepej et al., 2007; Zajkowska et al., 2011), strengthening a possible neuronal origin and clinical relevance of these two chemokines during flaviviral infections. In 2 small series of JE patients, CSF levels of CXCL10 were not been found to be raised (Kalita et al., 2010; Mahima et al., 2016). CXCL11 has not been investigated in JE patients thus far. Further investigations should be done on human CSF and brain autopsies to confirm the importance of CXCL10 and CXCL11 in JE.

In JE patients, IL8 and CCL5 were found to be elevated in the CSF and plasma. A positive correlation between fatality rate and IL8 levels was also reported (Singh et al., 2000; Winter et al., 2004). Our transcriptome results show that IL8 and CCL5 were among the highest upregulated chemokine genes in infected neurons and these cells may well be the source of these chemokines in the CSF. CCL5 expression has also been demonstrated in JEV-infected neuroglia and murine neuroblastoma cells (Chen et al., 2004; Gupta et al., 2010b). IFNB1 elevation has not been reported in JE patients. However, IFNB1 was highly upregulated in this study, suggesting that IFNB1 may also be involved in JE.

Previous understanding on neuronal innate immunity responses to JEV infection was mainly derived from murine neuronal cells and mouse models. In order to better investigate neuronal responses and account for species variation, human neuronal cell line, SK-N-MC was used in this study. Although of human origin, SK-N-MC is however a cancer cell line, derived from a supra-orbital metastatic site, therefore, the possibility of non-specific responses could not be excluded. Further investigations using primary human neuronal cells as well as CSF and brain autopsies should be done to confirm our findings.

5. Conclusion

The transcriptome profile in this study provides an overview on the global gene expressions induced by JEV infection in neurons, including important proinflammatory mediators RIG-1, MDA5 and CXCL11.

Acknowledgements

We thank Dr. Takasaki, NIID, Japan for the Jath-160 anti-JEV antibody used in this study. This work was supported by the HIR grant, University of Malaya, Malaysia [Project number: UM.C/625/1/HIR/MOHE/MED/06] and Postgraduate Research Fund, University of Malaya, Malaysia [Project number: PG285–2016A].

Appendix A. Supporting information

Supplementary data associated with this article can be found in the online version at doi:10.1016/j.virol.2018.10.015.

References

Babu, G.N., Kalita, J., Misra, U.K., 2006. Inflammatory markers in the patients of Japanese encephalitis. Neurol. Res. 28 (2), 190–192.
Bendall, L., 2005. Chemokines and their receptors in disease. Histol. Histopathol. 20 (3), 907–926.
Bhowmick, S., Duseja, R., Das, S., Appaiahgiri, M.B., Vrati, S., Basu, A., 2007. Induction of IP-10 (CXCL10) in astrocytes following Japanese encephalitis. Neurosci. Lett. 414 (1), 45–50.
Brazma, A., Hingamp, P., Quackenbush, J., Sherlock, G., Spellman, P., Stoeckert, C., et al., 2001. Minimum information about a microarray experiment (MIAME)—toward

standards for microarray data. Nat. Genet. 29 (4), 365–371.
Chen, C.-J., Chen, J.-H., Chen, S.-Y., Liao, S.-L., Raung, S.-L., 2004. Upregulation of RANTES gene expression in neuroglia by Japanese encephalitis virus infection. J. Virol. 78 (22), 12107–12119.
Cole, K.E., Strick, C.A., Paradis, T.J., Ogborne, K.T., Loetscher, M., Gladue, R.P., et al., 1998. Interferon–inducible T cell alpha chemoattractant (I-TAC): a novel Non-ELR CXC Chemokine with potent activity on activated T cells through selective high affinity binding to CXCR3. J. Exp. Med. 187 (12), 2009–2021.
Errett, J.S., Suthar, M.S., McMillan, A., Diamond, M.S., Gale, M., 2013. The essential, nonredundant roles of RIG-I and MDA5 in detecting and controlling West Nile virus infection. J. Virol (JVI. 01488-01413).
Fadnis, P.R., Ravi, V., Desai, A., Turtle, L., Solomon, T., 2013. Innate immune mechanisms in Japanese encephalitis virus infection: effect on transcription of pattern recognition receptors in mouse neuronal cells and brain tissue. Viral Immunol. 26 (6), 366–377.
Fredericksen, B.L., Keller, B.C., Fornek, J., Katze, M.G., Gale, M., 2008. Establishment and maintenance of the innate antiviral response to West Nile Virus involves both RIG-I and MDA5 signaling through IPS-1. J. Virol. 82 (2), 609–616.
German, A.C., Myint, K.S.A., Mai, N.T.H., Pomeroy, I., Phu, N.H., Tzartos, J., Barrett, A., 2006. A preliminary neuropathological study of Japanese encephalitis in humans and a mouse model. Trans. R. Soc. Trop. Med. Hyg. 100 (12), 1135–1145.
Gupta, N., Lomash, V., Rao, P.L., 2010a. Expression profile of Japanese encephalitis virus induced neuroinflammation and its implication in disease severity. J. Clin. Virol. 49 (1), 4–10.
Gupta, N., Santhosh, S.R., Babu, J.P., Parida M, M., Rao, P.L., 2010b. Chemokine profiling of Japanese encephalitis virus-infected mouse neuroblastoma cells by microarray and real-time RT-PCR: implication in neuropathogenesis. Virus Res. 147 (1), 107–112.
Gupta, N., Rao, P.L., 2011. Transcriptomic profile of host response in Japanese encephalitis virus infection. Virol. J. 8 (1), 92.
Henry Sum, M.S., 2015. The involvement of microtubules and actin during the infection of Japanese encephalitis virus in neuroblastoma cell line, IMR32. BioMed Res. Int. 2015.
Kalita, J., Srivastava, R., Mishra, M.K., Basu, A., Misra, U.K., 2010. Cytokines and chemokines in viral encephalitis: a clinicoradiological correlation. Neurosci. Lett. 473 (1), 48–51.
Kärber, G., 1931. Beitrag zur kollektiven Behandlung pharmakologischer Reihenversuche. Naunyn-Schmiede. Arch. Exp. Pathol. Pharmakol. 162 (4), 480–483.
Kato, H., Takeuchi, O., Sato, S., Yoneyama, M., Yamamoto, M., Matsui, K., et al., 2006. Differential roles of MDA5 and RIG-I helicases in the recognition of RNA viruses. Nature 441 (7089), 101.
Klein, R.S., Lin, E., Zhang, B., Luster, A.D., Tollett, J., Samuel, M.A., et al., 2005. Neuronal CXCL10 directs CD8+ T-cell recruitment and control of West Nile virus encephalitis. J. Virol. 79 (17), 11457–11466.
Kumar, M., Verma, S., Nerurkar, V.R., 2010. Pro-inflammatory cytokines derived from West Nile virus (WNV)-infected SK-N-SH cells mediate neuroinflammatory markers and neuronal death. J. Neuroinflamm. 7 (1), 73.
Lampron, A., ElAli, A., Rivest, S., 2013. Innate immunity in the CNS: redefining the relationship between the CNS and Its environment. Neuron 78 (2), 214–232.
Lepej, S.Z., Mišić-Majerus, L., Jeren, T., Rode, O., Remenar, A., Šporec, V., Vince, A., 2007. Chemokines CXCL10 and CXCL11 in the cerebrospinal fluid of patients with tick-borne encephalitis. Acta Neurol. Scand. 115 (2), 109–114.
Libraty, D.H., Nisalak, A., Endy, T.P., Suntayakorn, S., Vaughn, D.W., Innis, B.L., 2002. Clinical and immunological risk factors for severe disease in Japanese encephalitis. Trans. R. Soc. Trop. Med. Hyg. 96 (2), 173–178.
Livak, K.J., Schmittgen, T.D., 2001. Analysis of relative gene expression data using real-time quantitative PCR and the $2^{-\Delta\Delta CT}$ method. Methods 25 (4), 402–408.
Loo, Y.-M., Gale, M., 2011. Immune signaling by RIG-I-like receptors. Immunity 34 (5), 680–692.
Mahima, M., Mohammed, J., Shahla, A., Ashok, K., 2016. Cytokines profile in JE and non JE encephalitis. Int. J. Sci. Res. 5 (2), 1112–1117.
Misra,, U.K., Kalita, J., 2010. Overview: japanese encephalitis. Prog. Neurobiol. 91 (2), 108–120.
Mogensen, T.H., 2009. Pathogen recognition and inflammatory signaling in innate immune defenses. Clin. Microbiol. Rev. 22 (2), 240–273.
Nasirudeen, A.M.A., Wong, H.H., Thien, P., Xu, S., Lam, K.-P., Liu, D.X., 2011. RIG-I, MDA5 and TLR3 synergistically play an important role in restriction of dengue virus infection. PLoS Negl. Trop. Dis. 5 (1), e926.
Nazmi, A., Dutta, K., Basu, A., 2011. RIG-I mediates innate immune response in mouse neurons following Japanese encephalitis virus infection. PLoS One 6 (6), e21761.
Pirooznia, M., Nagarajan, V., Deng, Y., 2007. GeneVenn-A web application for comparing gene lists using Venn diagrams. Bioinformation 1 (10), 420.
Ravi, V., Parida, S., Desai, A., Chandramuki, A., Gourie-Devi, M., Grau, G.E., 1997. Correlation of tumor necrosis factor levels in the serum and cerebrospinal fluid with clinical outcome in Japanese encephalitis patients. J. Med. Virol. 51 (2), 132–136.
Schoepp, R.J., Beaty, B.J., 1984. Titration of dengue viruses by immunofluorescence in microtiter plates. J. Clin. Microbiol. 20 (5), 1017–1019.
Singh, A., Kulshreshtha, R., Mathur, A., 2000. Secretion of the chemokine interleukin-8 during Japanese encephalitis virus infection. J. Med. Microbiol. 49 (7), 607–612.
Solomon, T., Vaughn, D.W., 2002. Pathogenesis and clinical features of Japanese encephalitis and West Nile virus infections. In: Japanese Encephalitis and West Nile Viruses. Springer, Berlin, Heidelberg, pp. 171–194.
Tiroumourougane, S.V., Raghava, P., Srinivasan, S., 2002. Japanese viral encephalitis. Postgrad. Med. J. 78 (918), 205–215.
Unni, S.K., Růžek, D., Chhatbar, C., Mishra, R., Johri, M.K., Singh, S.K., 2011. Japanese encephalitis virus: from genome to infectome. Microbes Infect. 13 (4), 312–321.
Venter, M., Myers, T.G., Wilson, M.A., Kindt, T.J., Paweska, J.T., Burt, F.J., et al., 2005. Gene expression in mice infected with West Nile virus strains of different neurovirulence. Virology 342 (1), 119–140.
WHO, 2015, December 2015. Japanese encephalitis. Retrieved Jun, 2017, 2017, from ⟨http://www.who.int/mediacentre/factsheets/fs386/en/⟩.
Winter, P.M., Dung, N.M., Loan, H.T., Kneen, R., Wills, B., Thu, L.T., et al., 2004. Proinflammatory cytokines and chemokines in humans with Japanese encephalitis. J. Infect. Dis. 190 (9), 1618–1626.
Wong, K.T., Ng, K.Y., Ong, K.C., Ng, W.F., Shankar, S.K.,, Mahadevan, A., et al., 2012. Enterovirus 71 encephalomyelitis and Japanese encephalitis can be distinguished by topographic distribution of inflammation and specific intraneuronal detection of viral antigen and RNA. Neuropathol. Appl. Neurobiol. 38 (5), 443–453.
Zajkowska, J., Moniuszko-Malinowska, A., Pancewicz, S.A., Muszyńska-Mazur, A., Kondrusik, M., Grygorczuk, S., Czupryna, P., 2011. Evaluation of CXCL10, CXCL11, CXCL12 and CXCL13 chemokines in serum and cerebrospinal fluid in patients with tick borne encephalitis (TBE). Adv. Med. Sci. 56 (2), 311–317.